Title

Deep-ocean circulation in the North Atlantic during the Plio-Pleistocene intensification of Northern Hemisphere Glaciation (~2.65–2.4 Ma)

Authors

Kim A. Jakob[a], Jörg Pross[a], Jasmin M. Link[b], Patrick Blaser[a,c], Anna Hauge Braaten[d], Oliver Friedrich[a]

[a]Institute of Earth Sciences, Heidelberg University, Im Neuenheimer Feld 234–236, 69120 Heidelberg, Germany

[b]Institute of Environmental Physics, Heidelberg University, Im Neuenheimer Feld 229, 69120 Heidelberg, Germany

[c]Institute of Earth Sciences, University of Lausanne, Géopolis, 3893, 1015 Lausanne, Switzerland

[d]Bjerknes Centre for Climate Research and Department of Earth Science, University of Bergen, Allegaten 41, 5007 Bergen, Norway

Corresponding author

K.A. Jakob, Institute of Earth Sciences, Heidelberg University, Im Neuenheimer Feld 234–236, 69120 Heidelberg, Germany (kim.jakob@geow.uni-heidelberg.de)

Abstract

Through transporting heat around the world and thereby regulating global climate, ocean circulation is an integral part of Earth's climate system that likely changed substantially on glacial-interglacial timescales in the deep North Atlantic Ocean. However, quantitative records on deep-water dynamics in the North Atlantic older than ~1 Myr are sparse and typically of low temporal resolution. Here we provide a new record on northern- versus southern-sourced waters in the deep North Atlantic at a yet unprecedented temporal resolution. Our record is based on a novel approach (Atlantic-Pacific bottom-water temperature (BWT) difference) for an interval comprising the onset of larger-scale glaciations in the Northern Hemisphere, the Plio-Pleistocene transition (~2.65–2.4 Ma; Marine Isotope Stages G1–95). We thus have generated a new, millennial-scale-resolution BWT record based on benthic foraminiferal Mg/Ca from Ocean Drilling Program Site 849 in the East Pacific backed up with a new neodymium-isotope record on glacial-interglacial-scale resolution. The difference between our new BWT record (Site 849) and previously available BWTs from Integrated Ocean Drilling Program Site U1313 in the North Atlantic was used to decipher changes between southern- and northern-sourced waters in the deep North Atlantic. In accordance with previous studies, we document an increased influence of deep waters from high southern latitudes during glacials at the expense of northern-sourced waters. Perhaps even more importantly, our new record is highly relevant for the determination of geochemically-based sea-level records from the deep North Atlantic, which was yet limited by quantitative estimates of deep-water masses at a sufficient, (sub-)millennial-scale resolution.

Keywords

benthic foraminiferal Mg/Ca, Atlantic-Pacific bottom-water-temperature difference, neodymium isotopes, deep-ocean circulation, Plio-Pleistocene intensification of Northern Hemisphere Glaciation

1. Introduction

The Atlantic Meridional Overturning Circulation (AMOC) plays a prominent role in controlling global climate through regulating latitudinal heat transport and carbon sequestration between the atmosphere and the deep ocean (e.g. Raymo et al., 1998; Rahmstorf, 2002; Sigman et al., 2010; Henry et al., 2016). The deep Atlantic Ocean is presently bathed by two major water masses – one being formed in the northern part of the basin (northern-component waters (NCW), i.e., North Atlantic Deep Water (NADW)) and another one that derives from the south (southern-component waters (SCW), i.e., Antarctic Bottom Water (AABW)) (Fig. 1). Due to their different source regions, these water masses exhibit clear differences in their neodymium isotope (ε_{Nd}) and stable carbon isotope ($\delta^{13}C$) signatures (NADW: ε_{Nd} = -12.3, $\delta^{13}C$ = 1 ‰; AABW: ε_{Nd} = -8.6, $\delta^{13}C$ = 0.4 ‰ (Kroopnick, 1985; Tachikawa et al., 2017)). $\delta^{13}C$ records of deep-sea benthic foraminifera (e.g., Raymo et al., 1990; Lisiecki, 2014; Lang et al., 2016) as well as authigenic ε_{Nd} values of materials such as fish teeth or debris (e.g., Staudigel et al., 1985; Martin & Haley, 2000; Frank, 2002; Lang et al., 2016) are thus typically used as paleoceanographic proxies to trace ocean-circulation changes in the Atlantic Ocean and elsewhere.

As such, North Atlantic $\delta^{13}C$ proxy records are traditionally interpreted to document the penetration of southern-sourced deep waters into the North Atlantic at the expense of deep waters derived from the north during prominent glacials since the intensification of Northern Hemisphere Glaciation (iNHG) ~2.5 Ma ago (e.g., Raymo et al., 1990; Keigwin 2004; Curry and Oppo, 2005; Lang et al., 2016) ("changing mode" in Fig. 1a). This traditional, $\delta^{13}C$-derived view is supported by i) a North Atlantic ε_{Nd} record for the iNHG (Lang et al., 2016), and by ii) North Atlantic ε_{Nd} data (Böhm et al., 2015; Lang et al., 2016) together with $^{231}Pa/^{230}Th$ ratios, i.e., a measure of overall AMOC strength (Böhm et al., 2015), across the last glacial cycle. However, other records on ε_{Nd} (Howe et al., 2016; Pöppelmeier et al., 2020) suggest that southern-sourced waters possibly did not expand farther into the deep North Atlantic during the Last Glacial Maximum than today ("constant mode" in Fig. 1b).

1.2 Importance of high-resolution records on water-mass prevalence in the deep North Atlantic Ocean

Profound knowledge on deep-ocean dynamics is not only relevant for our understanding of the Earth's climate system, but also of particular importance for sea-level reconstructions based on benthic geochemical proxy records. This is because water masses not only differ in their ε_{Nd} and $\delta^{13}C$ signatures, but also with regard to other parameters such as temperature or the seawater oxygen-isotope composition ($\delta^{18}O_{sw}$). The latter, in turn, influence for example the Mg/Ca ratio and the stable oxygen isotope ($\delta^{18}O$) composition of benthic foraminifers – proxy records commonly used to evaluate past sea-level change.

To date, a correction for such records is limited by the lack of quantitative estimates of the prevailing water mass at a sufficient (i.e., [sub-]millennial-scale) temporal resolution. Among those estimates that are yet available (e.g., Raymo et al., 1990, 1992; Lang et al., 2016), the $\delta^{13}C$-based record of northern-component waters (%NCW) from Lang et al. (2016) for Integrated Ocean Drilling Program (IODP) Site U1313 in the North Atlantic has the highest temporal resolution (~4 kyr). That record covers the Plio-Pleistocene iNHG, but applying it to higher-resolution (sub-millennial-scale) benthic Mg/Ca and $\delta^{18}O$ data of the same site and time interval (Jakob et al., 2020) results in a clear overestimate of absolute glacial sea-level lowstand values compared to yet available sea-level records (e.g., mean value of ~135 m below modern (Jakob et al., 2020) versus a maximum of ~60 m below modern (e.g., de Boer et al., 2014; Miller et al., 2020) for Marine Isotope Stage (MIS) 100).

The above clearly highlights the need for improving our knowledge on the water-mass mixing history in the deep North Atlantic Ocean. This is even more true in light of anthropogenic climate change, which requires a better understanding of sea-level dynamics under warmer-than-modern climatic conditions, such as during the Plio-Pleistocene, on human-relevant timescales. To derive such geochemically-based sea-level reconstructions, in turn, profound knowledge on the deep water-mass mixing history at a sub-millennial-scale resolution is required. This is because high-resolution records on water-mass mixing (compared to yet available lower resolved records) are likely more appropriate to be integrated with well-resolved benthic geochemical proxy records from North Atlantic drill cores for sea-level reconstruction.

1.3 Atlantic-Pacific bottom-water temperature difference as a tracer for North Atlantic deep-water masses

To improve our understanding of water-mass prevalence in the deep North Atlantic, we generated a new, semi-quantitative record of the deep-water mixing history in the North Atlantic (%NCW) for ~2.65 to 2.4 Ma (MIS G1–95) at a yet unprecedented temporal resolution. Our record is based on a novel approach utilizing the difference in Atlantic-Pacific bottom-water-temperatures (ΔBWT) derived from benthic foraminiferal calcite. It covers the late Pliocene/early Pleistocene, including the culmination of the iNHG (MIS 100–96). During that time, the Laurentide Ice Sheet advanced into the midlatitudes for the first time (Bailey et al., 2010; Balco and Rovey, 2010; Lang et al., 2014), and ice rafting became widespread across the North Atlantic (e.g., Shackleton et al., 1984; Flesche Kleiven et al., 2002; Naafs et al., 2013), with ice-rafted debris flux and provenance comparable to that of the Last Glacial Maximum (Bailey et al., 2013).

Traditionally, benthic $\delta^{13}C$ gradients are used for the purpose of our study – an approach we did not select here because benthic $\delta^{13}C$ is likely not a simple fingerprint of water masses, but is also affected by other geochemical processes, such as organic-matter remineralization, that can substantially alter the initial $\delta^{13}C$ signature of a water mass (e.g., Gebbie, 2014). This might be of particular relevance for high-productivity regions such as the Eastern Equatorial

Pacific (EEP), where the benthic $\delta^{13}C$ signal likely reflects both the water-mass signature and local variations in productivity and therefore organic-matter export into and remineralization in the deep sea (Jakob et al., 2016).

To determine Atlantic-Pacific ΔBWT, we choose a site in the North Atlantic (IODP Site U1313) that was alternately bathed by cold, southern-derived waters during glacials and warmer, northern-sourced deep waters during interglacials as evidenced by both ε_{Nd} and $\delta^{13}C$ records (e.g., Raymo et al., 1990; Dwyer and Chandler, 2008; Lang et al., 2016). In contrast, our selected Pacific Ocean site (Ocean Drilling Program (ODP) Site 849) was consistently bathed by relatively cold, southern-sourced waters (Mix et al., 1995) (Fig. 2). Importantly, deep-water formation in the North Pacific and export to the lower latitudes as considered for the warm Pliocene (Burls et al., 2017; Ferreira et al., 2018) or late Pleistocene extreme glacials (Knudson & Ravelo, 2015) is unlikely to have occurred during our target interval.

For Site 849, a new, millennial-scale resolution BWT record has been generated for this study, while for Site U1313 such a record is already available (Jakob et al., 2020) (Tab. 1). Based on these records, our approach relies on the simple approximation that a large BWT difference between these sites indicates northern-sourced waters in the deep North Atlantic, while a reduced BWT difference suggests the penetration of southern-sourced deep waters into the North Atlantic (see Section 2.6 for details). The fidelity of our approach is validated with new (Site 849) and previously available (Site U1313; Lang et al., 2016) ε_{Nd} data as a tracer for different water masses from both the East Pacific and the North Atlantic Oceans (Tab. 1).

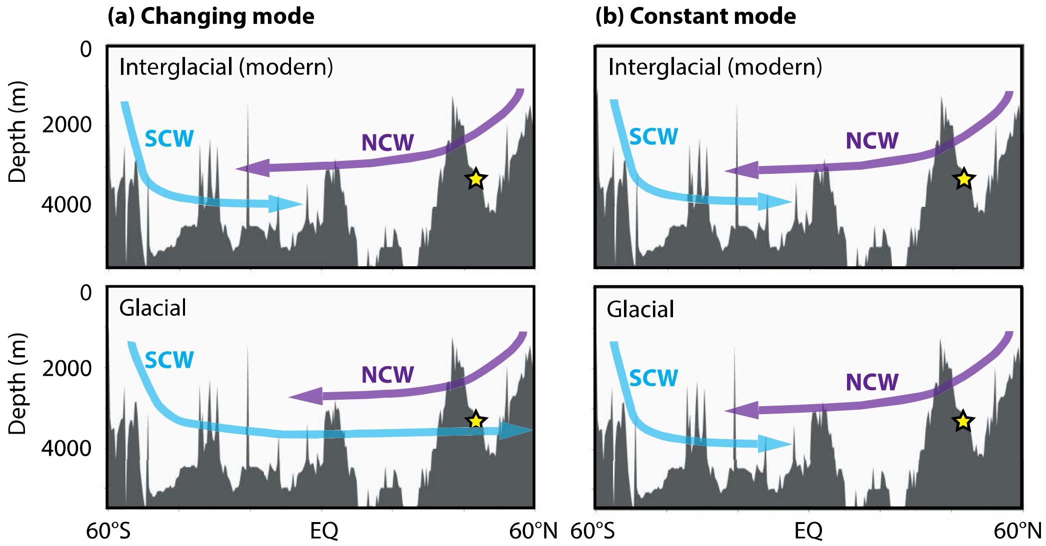

Figure 1. Schematic illustration of deep-water masses in the Atlantic Ocean. Blue and purple arrows indicate the pathway of southern- and northern-component waters (SCW and NCW, respectively) for both interglacials and glacials in two different scenarios. (a) "Changing mode" with SCW penetrating further north during glacials compared to interglacials. (b) "Constant mode" with no significant changes in deep-water circulation on the glacial-interglacial timescale. Yellow star indicates the position of IODP Site U1313. The north-south depth profile corresponds to 32 °W as indicated in Fig. 2a. Bathymetry after Ocean Data View (Schlitzer, 2016).

2. Material and methods

2.1. Site locations

The following two sites were used to evaluate the Atlantic-Pacific BWT difference and thus water-mass prevalence in the deep North Atlantic: ODP Site 849 (0.1°N, 110.3°W, 3851 m water depth; Mayer et al. (1992)) in the EEP and IODP Site U1313 (41.0°N, 32.6°W, 3426 m water depth; Expedition 306 Scientists (2006)) in the North Atlantic (Fig. 2). Site 849 has been chosen because (i) it was permanently bathed by a single deep-water mass derived from the south (see Section 1.3), (ii) it can be considered to represent mean Pacific Ocean conditions (Mix et al., 1995) and (iii) it exhibits continuous sedimentation with high sedimentation rates (2.5–3 cm/kyr (Mayer et al., 1992; Mix et al., 1995; Jakob et al., 2017)) and good foraminiferal preservation (Jakob et al., 2016; Jakob et al., 2018) throughout our study interval. Site U1313 has been selected because (i) it was under the varying influence of NCW and SCW during Plio-

Pleistocene interglacials and glacials, respectively (e.g., Raymo et al., 1990; Lang et al., 2016), and (ii) it is the reoccupation of Deep Sea Drilling Program (DSDP) Site 607, a benchmark site for monitoring deep waters throughout the Plio-Pleistocene, that benefited from modern coring techniques (Expedition 306 Scientists, 2006, and references therein).

Both sites exhibit excellent age control for the study interval owing to their high-resolution benthic foraminiferal (*Cibicidoides wuellerstorfi*) $\delta^{18}O$ chronologies tuned to the LR04 stack (Lisiecki and Raymo, 2005; Bolton et al., 2010; Jakob et al., 2017). Together, these details warrant optimum preconditions for generating a high-quality, semi-quantitative record of the water-mass provenance in the North Atlantic Ocean at a high temporal resolution.

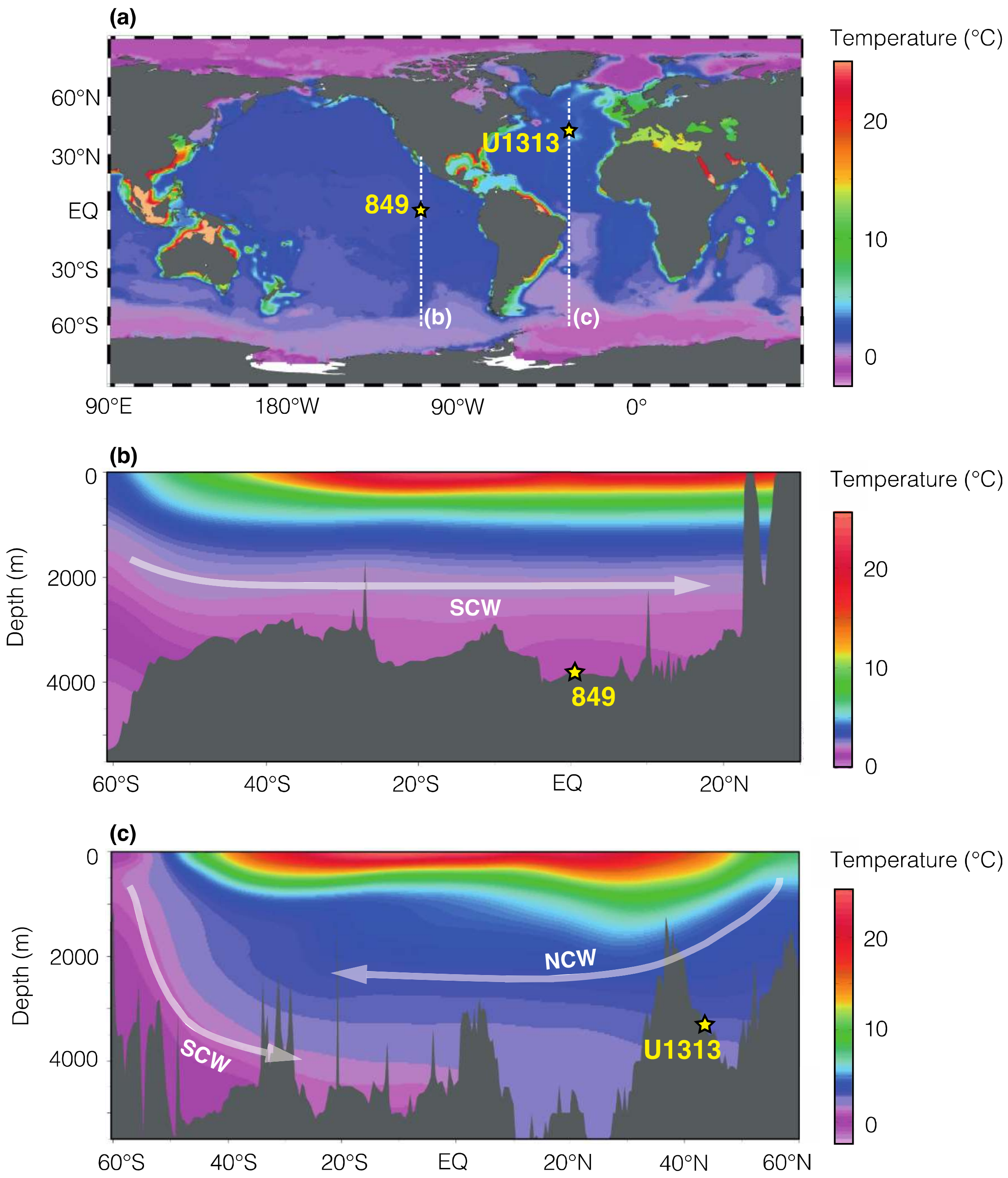

Figure 2. Location of studied sites. (a) Global map showing the position of ODP Site 849 in the East Pacific and IODP Site U1313 in the North Atlantic together with present-day mean annual sea-floor temperatures. Dashed lines indicate north-south depth profiles through the Pacific (110 °W) and Atlantic (32 °W) Oceans shown in (b) and (c), respectively. White arrows indicate the present-day pathway of southern-component waters (SCW) and northern-component waters (NCW). Bathymetry and temperatures (in °C) after Ocean Data View (Schlitzer, 2016) and World Ocean Atlas (Boyer et al., 2013; Locarnini et al., 2013).

2.2 Sample material and processing

For our study, a new benthic foraminiferal Mg/Ca-based BWT record on millennial-scale resolution together with a glacial-interglacial-scale resolution ε_{Nd} record have been generated for EEP Site 849 for the ~2.65–2.4 Ma interval. These records were then integrated with already available BWT and ε_{Nd} records of North Atlantic Site U1313 (Lang et al., 2016; Jakob et al., 2020) (Tab. 1).

To study MIS G1–95 (~2.65–2.4 Ma) at Site 849, we investigated cores 849C-7H-1-80 cm to 849C-7H-2-21 cm and 849D-6H-5-102 cm to 849D-7H-3-73 cm (67.8–74.2 m composite depth (mcd); Hagelberg et al., 1992). For generating a record on a millennial-scale temporal resolution, 190 samples (sample volume: 20 cm^3) were investigated at a 2-cm spacing, which yields a temporal resolution of ~800 yr (Jakob et al., 2017).

For foraminiferal Mg/Ca analysis, samples were dried, weighed, and washed over a 63 µm sieve. On average, twelve tests of the benthic foraminifer *Oridorsalis umbonatus* (Reuss, 1851) (Fig. 3) were picked from the >150 µm dried sediment fraction of these samples. Subsequently, tests were cracked and homogenized; a subsample of ~2/3 was used for Mg/Ca analysis. The species *O. umbonatus* was selected for our study because it occurs continuously throughout the studied core material with the necessary number of individuals; further it is well suited for the purpose of our study as it is a highly reliable Mg/Ca recorder. This is because (i) it is easier to clean for Mg/Ca analyses than other taxa due to its larger chambers, (ii) because of its shallow infaunal habitat it is well buffered to the influence of changes in seawater carbonate ions and thus ocean *pH* related to different water masses (Rathmann and Kuhnert, 2008; Lear et al., 2015), and (iii) it shows only a low sensitivity to temporal variations in seawater Mg/Ca (Mg/Ca_{sw}) (Lear et al., 2015). Importantly, the Mg/Ca-derived BWT record from Site U1313 (Jakob et al. 2020), to which we compare our new Mg/Ca-based BWT record from Site 849, is based on the same benthic foraminiferal species.

Table 1. Compilation of the geochemical datasets from ODP Site 849 and IODP Site U1313 evaluated in this study.

Site	Proxy record	Proxy for	Reference
ODP Site 849	Mg/Ca (*O. umbonatus*)	BWT	This study
	ε_{Nd} (fish debris)	Ocean circulation	This study
	$\delta^{18}O$ (*C. wuellerstorfi*)	Age model	Jakob et al. (2017)
IODP Site U1313	Mg/Ca (*O. umbonatus*)	BWT	Jakob et al. (2020)
	ε_{Nd} (fish debris)	Ocean circulation	Lang et al. (2016)
	$\delta^{18}O$ (*C. wuellerstorfi*)	Age model	Bolton et al. (2010)

2.3 Foraminiferal preservation

The preservation of the *O. umbonatus* tests used for Mg/Ca analysis was examined by Scanning Electron Microscopy (SEM) for selected specimens from both glacial and interglacial intervals. Images were taken with a LEO 440 SEM at the Institute of Earth Sciences, Heidelberg University. Results indicate that the preservation is consistently good to acquire high-quality Mg/Ca data (Fig. 3), which is in line with previous studies documenting excellent preservation of foraminiferal calcite for the studied interval of Site 849 (Jakob et al., 2016; Jakob et al., 2018).

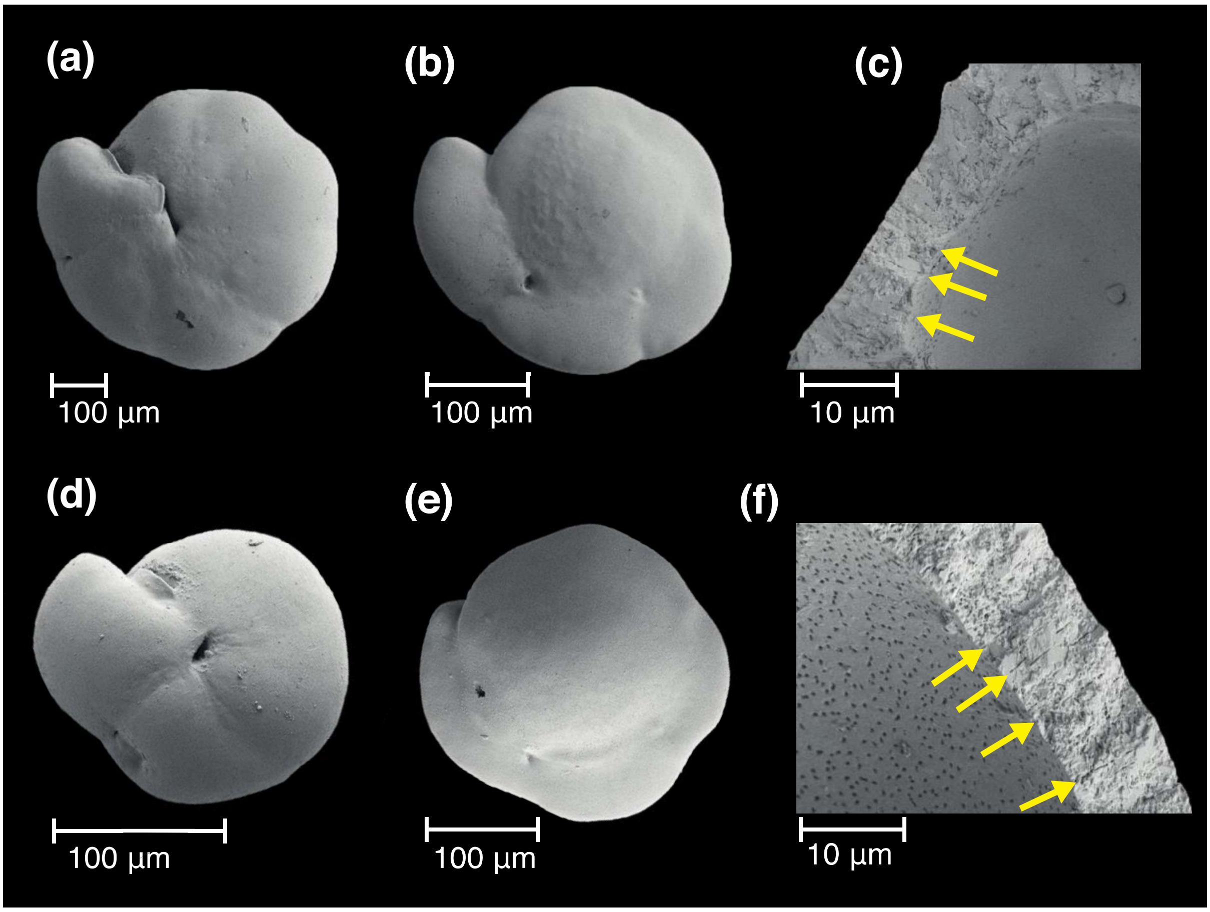

Figure 3. Scanning Electron Microscope micrographs of *Oridorsalis umbonatus* from Site 849 in the EEP. Both glacial (a–c; sample 849D-7H-2-41–43 cm) and interglacial (d–f; sample 849D-7H-4-103–105 cm) tests are well preserved, allowing for the acquisition of reliable Mg/Ca data. Note the preservation of delicate pore channels in the close-up views (yellow arrows in c, f).

2.4 Mg/Ca analysis

Samples for Mg/Ca analyses from Site 849 were carefully cleaned to remove clay minerals, organic material and re-adsorbed contaminants following the cleaning protocol from Barker et al. (2003). The reductive cleaning step was omitted because it removes Mg from foraminiferal tests and therefore decreases their Mg/Ca ratios (Barker et al., 2003; Rosenthal et al., 2004).

Mg/Ca samples were run on an Agilent Inductively Coupled Plasma-Optical Emission Spectrometer (ICP-OES) 720 at the Institute of Earth Sciences, Heidelberg University. To identify potential contamination by clay particles or diagenetic coatings that might bias foraminiferal Mg/Ca ratios (Barker et al., 2003), the element ratios of Al/Ca, Fe/Ca and Mn/Ca were screened (see Section 3.1 for details). Reported Mg/Ca values were normalized relative to the ECRM 752-1 reference values of 3.762 mmol/mol (Greaves et al., 2008). Al/Ca, Fe/Ca, and Mn/Ca ratios are presented as unnormalized values since Al, Fe and Mn concentrations of the ECRM were typically below the detection limit of the ICP-OES (<1 mg/l); the fidelity of values derived for these elements, however, has been ensured with additional certified reference materials (SPS-SW2, TMDA-70.2). To ensure instrumental precision, the ECRM standard was monitored as an internal consistency standard at least every 20 samples. Based on these replicate measurements, the standard deviation for Mg/Ca is ±0.8 % (equal to approximately ±0.1 °C).

2.5 Paleotemperature reconstruction

Site 849 Mg/Ca ratios were converted into BWT estimates applying the same calibration used to reconstruct BWTs out of Mg/Ca data for Site U1313 (Jakob et al., 2020), i.e., a species-specific equation for *O. umbonatus* derived from core-top samples ($BWT = \ln [(Mg/Ca) / (1.008 \pm 0.08)] \times [1 / (0.114 \pm 0.02)]$) (Lear et al., 2002). Based on error propagation including both the uncertainty of the Mg/Ca analysis and of the BWT calibration, we estimate the uncertainty for our BWT estimates to be ±0.8 °C.

Reasons for selecting the Mg/Ca-BWT calibration from Lear et al. (2002) for our study are three-fold: First, it is an *O. umbonatus*-specific calibration, and the Mg/Ca values that we reconstruct for Site 849 (0.95–1.96 mmol/mol) fit best to the calibration range (1.09–3.43 mmol/mol) of that equation compared to other species-specific equations (Fig. 4). Temperatures in our reconstruction for the 0.95–1.09 mmol/mol Mg/Ca range might be more uncertain than those for the 1.09–1.96 mmol/mol range, but the same uncertainty would also derive from all other yet available *O. umbonatus*-specific Mg/Ca-temperature calibrations. Second, proper

BWT-difference calculation between North Atlantic Site U1313 and EEP Site 849 requires that BWT records from both sites are based on the same Mg/Ca-BWT calibration, and the only yet available *O. umbonatus*-specific calibration that captures nearly the entire Mg/Ca range reconstructed for Sites 849 and U1313 (0.95–3.32 mmol/mol) is that from Lear et al. (2002) (Fig. 4). Third, the selected equation is based on multiple, globally distributed core-top samples and therefore applicable to both the EEP and the North Atlantic Oceans.

Applying the above calibration to our Mg/Ca data from Site 849 requires two adjustments: First, because the selected equation is based on oxidative and reductive cleaning of foraminiferal tests, while we only applied oxidative cleaning to our samples, the measured Mg/Ca values were adjusted by reducing each value by 10 % (Barker et al., 2003; Ford et al., 2016). Second, Mg/Ca values used for our BWT reconstruction were adjusted to past variations in Mg/Ca_{sw} by using equation (3) from Lear et al. (2002) and estimates of past Mg/Ca_{sw} from Evans et al. (2016). This correction is required because temporal variations in Mg/Ca_{sw} from 5.2 mol/mol in the modern to 4.25–4.4 mol/mol during the studied interval (Evans et al., 2016) have the potential to influence reported foraminiferal Mg/Ca ratios (and therefore Mg/Ca-based records) of timescales longer or older than the residence time of Mg and Ca in seawater, i.e., >1 Myr (Fantle & DePaolo, 2005; 2006). Although uncertainties are associated with past Mg/Ca_{sw} estimates (compare, e.g., Evans et al. (2016) and Rausch et al. (2013)) and therefore with absolute BWTs that we calculate, the BWT difference is not affected by this source of uncertainty as the same Mg/Ca_{sw} estimates (Evans et al., 2016) are applied to the Site 849 and U1313 sample sets.

The above-described approach selected to calculate BWT at Site 849 was validated by reconstructing deep-sea temperatures for Holocene samples of the same site that were treated identically to the Plio-Pleistocene samples. Our exercise shows that the resulting temperature is, within the error associated with our approach, indistinguishable from the modern-day BWT at the study site of ~1.5 °C (Locarnini et al., 2013) (Fig. 5) and therefore justifies our calculations.

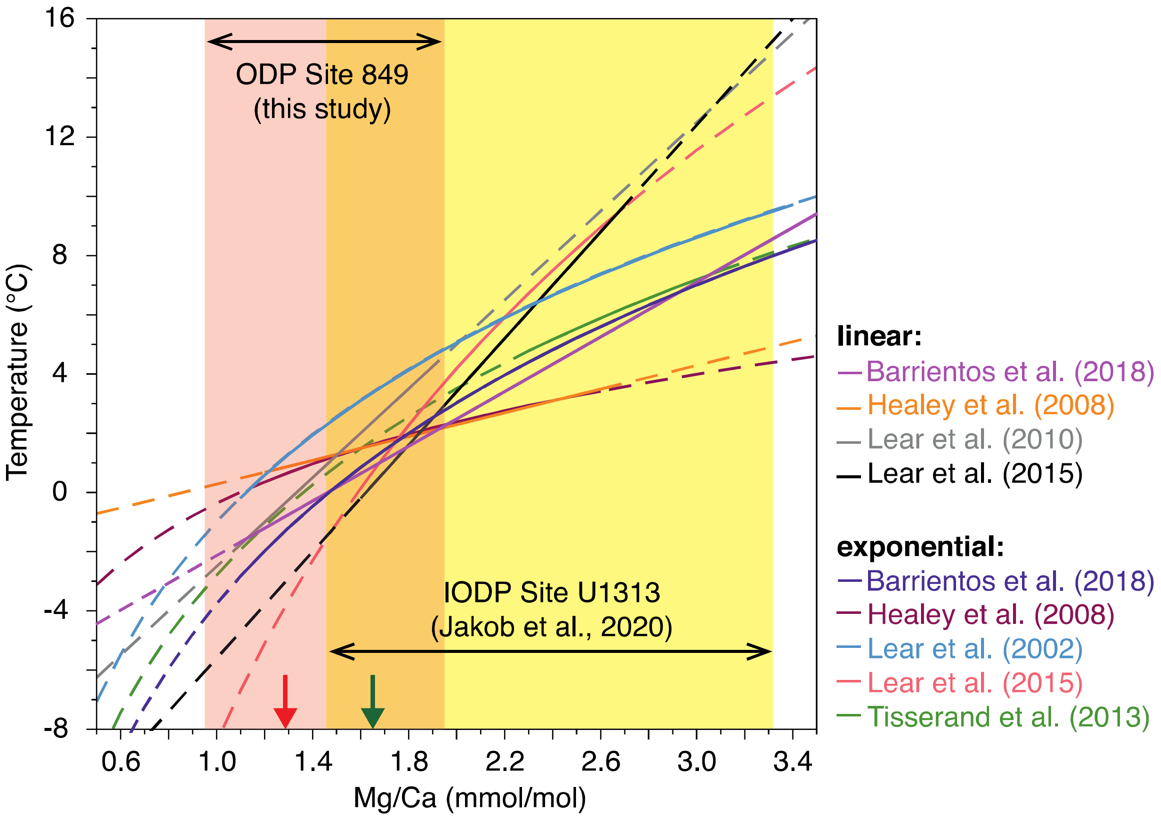

Figure 4. Species-specific Mg/Ca-BWT calibrations for *O. umbonatus*. Calibrations are from Lear et al. (2002) (used in this study), Healey et al. (2008), Lear et al. (2010), Tisserand et al., (2013), Lear et al. (2015), and Barrientos et al. (2018). Solid part of a line depicts the calibration range for each equation. Note that the calibration from Barrientos et al. (2018) is based on *O. tener* and *O. umbonatus*. Orange and yellow bars highlight the Mg/Ca raw-data range of O. *umbonatus* at Site 849 (this study) and Site U1313 (Jakob et al., 2020), respectively, for the herein studied time interval (~2.65–2.4 Ma). Red and green arrows indicate Mg/Ca values of most recent samples of ODP Site 849 (1.28 mmol/mol; this study) and IODP Site U1313 (1.53 mmol/mol; Jakob et al., 2020), respectively.

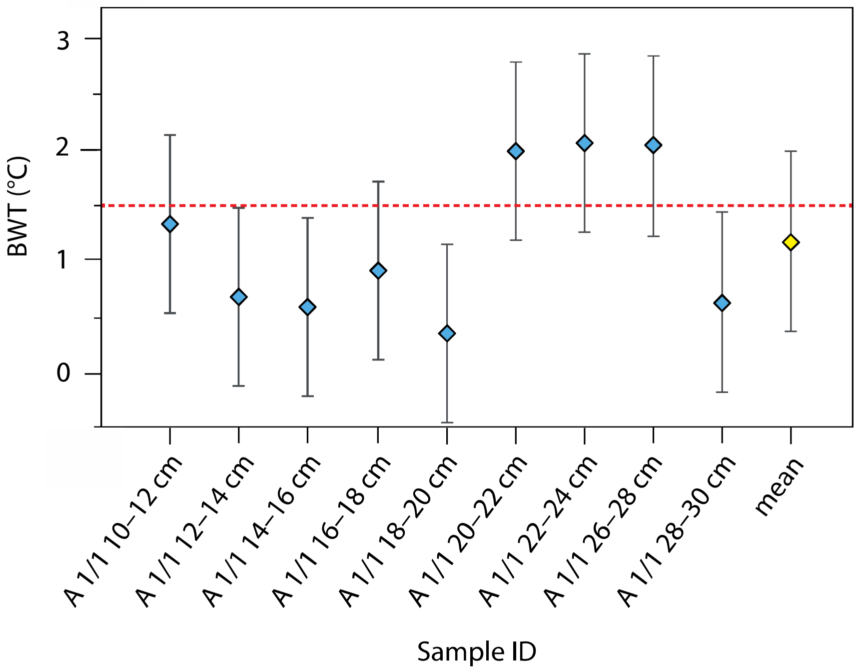

Figure 5. Mg/Ca-derived BWTs for uppermost (Holocene) samples from Site 849. Temperatures of nine samples (blue) and the from these samples resulting mean value (yellow) are shown in comparison to the present-day BWT at Site 849 (~1.5 °C (red dashed line); Locarnini et al., 2013). Vertical bars indicate the standard deviation (±1σ) associated with the reconstructed temperature values.

2.6 Calculation of the bottom-water temperature difference and %NCW

As highlighted above, both sample sets from North Atlantic Site U1313 (Jakob et al., 2020) and from EEP Site 849 (this study) were treated equally in terms of BWT calculation, which is a necessary precondition for a proper calculation of ΔBWT between these two sites. For this purpose, the BWT record from Site U1313 (Jakob et al., 2020) was linearly interpolated to our new BWT record from Site 849 as the latter has a lower mean temporal resolution.

To develop a semi-quantitative record of %NCW in the deep North Atlantic out of the Atlantic-Pacific (Site U1313-to-849) temperature difference, the following assumptions were made: (i) An Atlantic-Pacific BWT difference of 0 °C or less indicates that both sites were bathed by the same southern-sourced water mass, which is equal to 0 %NCW at Site U1313. (ii) A difference of 2.6 °C or more (equal to the temperature difference between modern AABW and NADW; Craig & Gordon, 1965) is related to 100 %SCW at Site 849 in the EEP and 100 %NCW at Site U1313 in the North Atlantic. Any value in between these ΔBWT endmembers is likely to reflect a mixture of southern- and northern-sourced deep waters in the North Atlantic. Given an uncertainty in the Site 849 and U1313 BWT records of ±0.8 °C (this study) and ±1.1 °C (Jakob et al., 2020), respectively, calculated ΔBWT and %NCW estimates are necessarily more uncertain for a small (compared to rather large) Site 849-to-U1313 temperature difference.

Importantly, our approach relies on the assumption that ΔBWT between NADW and AABW, regardless of the absolute temperature value, was similar during our study interval and the present-day. Finally, we note that the selected approach is a simplified approach as southern-sourced deep water in the EEP might not solely reflect AABW *sensu stricto*, but rather represents Pacific Deep Water, i.e., a mixture of AABW, recirculated NADW and Antarctic Intermediate Water (e.g., Mix et al., 1995; Kwiek & Ravelo, 1999). AABW, however, is considered as its main component (Johnson, 2008) and therefore justifies our approach as a valid endmember scenario.

2.7 Smoothing of records

In our study, we present both raw data and smoothed records. The latter were generated in order to remove short-term variabilities and to emphasis the overall trend of a record. Smoothing was carried out with a five-point running average using the AnalySeries software package version 2.0.8 (Paillard et al., 1996).

2.8 Neodymium isotopes

To determine the neodymium isotopic composition of samples representing peak glacial and interglacial conditions at Site 849, fish teeth and bones with a minimum weight of 150 µg were picked from the >63 µm size fraction of six samples. Fish-debris samples were cleaned in

MilliQ water through ultrasonification and dissolved in concentrated HCl prior to column chemistry. Dissolution and column chemistry were performed following standard procedures (Cohen et al., 1988; Pin et al., 1994). Neodymium isotope ratios ($^{143}Nd/^{144}Nd$) were analyzed with a Multi Collector-Inductively Coupled Plasma-Mass Spectrometer Thermo Fisher Neptune Plus at the Institute of Environmental Physics, Heidelberg University. Raw data were corrected to a $^{146}Nd/^{144}Nd$ ratio of 0.7219 with an exponential mass bias law and subsequently to the accepted $^{143}Nd/^{144}Nd$ ratio of 0.512115 for the bracketing JNdi-1 standard solutions (Tanaka et al., 2000). Presented Nd isotope ratios are reported as $\varepsilon_{Nd} = \{[(^{143}Nd/^{144}Nd_{sample})/(^{143}Nd/^{144}Nd_{CHUR})]-1\} \times 10^4$, where $^{143}Nd/^{144}Nd_{CHUR}$ (value of 0.512638) refers to the Chondritic Uniform Reservoir (Jacobsen and Wasserburg, 1980). The reproducibility obtained from repeated measurements of secondary standards was ±0.2 ε_{Nd} units (2σ).

3. Results and discussion

3.1 Evaluation of contamination and diagenetic effects on Mg/Ca ratios of *O. umbonatus*

Al/Ca, Fe/Ca and Mn/Ca ratios of foraminiferal tests exceeding 0.1 mmol/mol are typically considered to indicate the presence of clay, Fe-Mn-oxyhydroxides or Fe-Mn carbonate coatings not removed during the Mg/Ca cleaning process. Such contaminations might bias the reconstructed Mg/Ca signature of foraminiferal tests (Barker et al., 2003).

In our samples, absolute Al concentrations were below or near the detection limit of the ICP-OES (see Section 2.4), which indicates that *O. umbonatus* tests were unaffected by clay contamination. Fe/Ca ratios remain typically below 0.1 mmol/mol, implying that Fe-bearing coatings did not exist on *O. umbonatus* test surfaces (Fig. 6a, c). In contrast, Mn/Ca values are clearly above the 0.1 mmol/mol threshold value indicative for the presence of Mn-rich coatings (Fig. 6b, c). This could have biased the Mg/Ca values of *O. umbonatus* that we report, because Mn-rich coatings also contain Mg that pushes the original test Mg/Ca signature towards higher values, leading to an overestimation of reconstructed temperatures (Barker et al., 2003; Hasenfratz et al., 2017).

However, in our samples we find no correlation between Mg/Ca and Mn/Ca ($r^2 = 0.005$) as it would be expected if tests were overgrown by Mn-rich coatings. For example, highest Mg/Ca ratios in our record of up to 1.96 mmol/mol at 2.63 Ma (corresponding to MIS G1) are not associated with enhanced Mn/Ca ratios (Fig. 6c), but rather reflect the average Mn/Ca ratio in our record (1.02 mmol/mol). Moreover, SEM images do not show any kind of microcrystalline overgrowth on *O. umbonatus* test surfaces (Fig. 3). Although we cannot entirely rule out the possibility of diagenetic changes in *O. umbonatus* tests because of enriched Mn/Ca ratios, we conclude that early diagenetic overprinting, if existing, has not severely affected Mg/Ca ratios of *O. umbonatus* for the ~2.65–2.4 Ma interval at Site 849 and therefore the interpretation of our record.

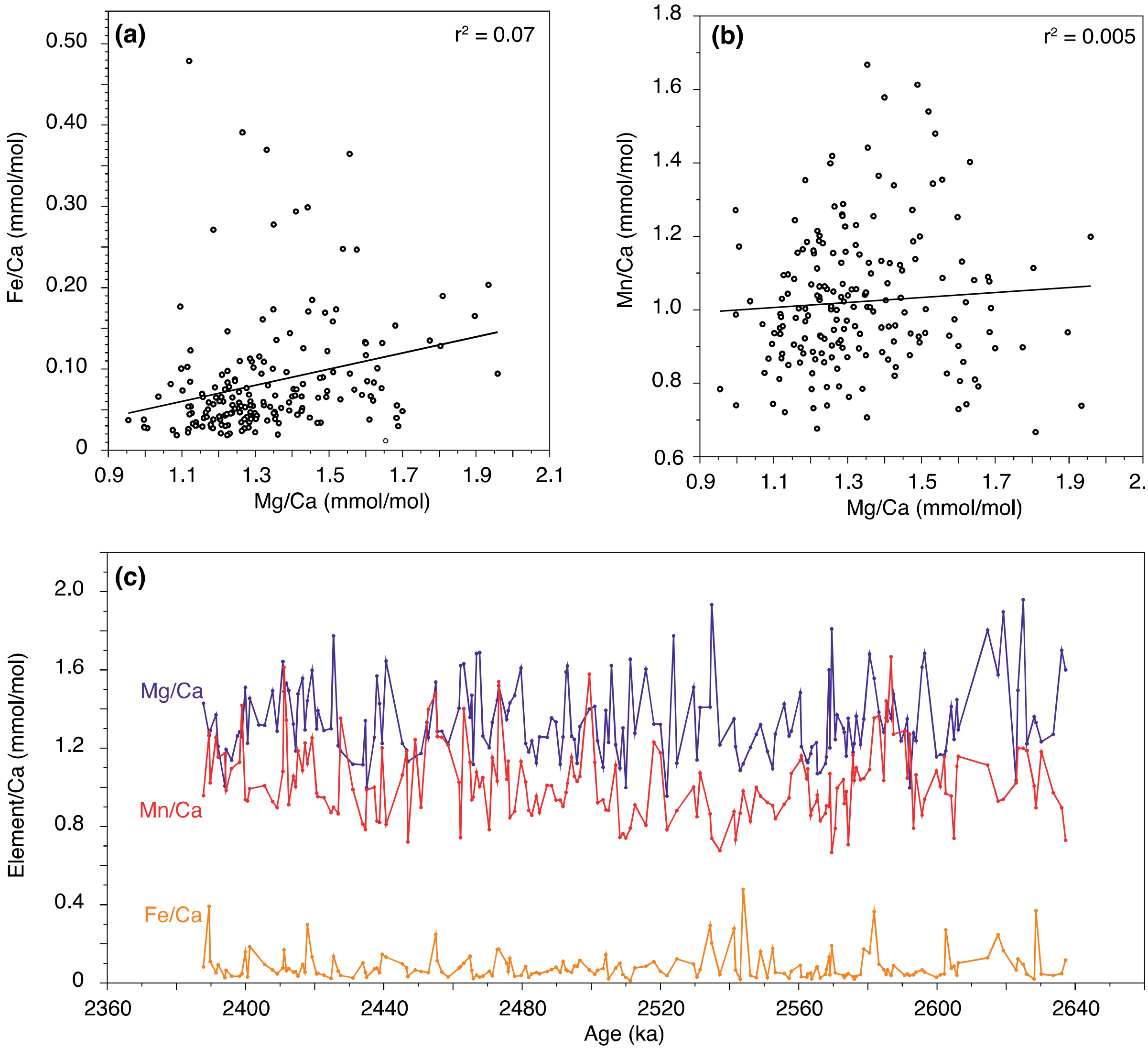

Figure 6. Evaluation of potential contaminations on the Mg/Ca ratio for *O. umbonatus* at Site 849 for the interval ~2.65–2.4 Ma. (a) Cross plot between Mg/Ca and Fe/Ca ratios. (b) Cross plot between Mg/Ca and Mn/Ca ratios. (c) Downcore Mg/Ca (dark blue), Mn/Ca (red) and Fe/Ca (orange) ratios.

3.2 Deep-water temperatures of the late Pliocene/early Pleistocene

3.2.1 East Pacific Site 849

The five-point smoothed average of our new Mg/Ca-based BWT record from Site 849 varies between 1.7 °C and 4.7 °C during the studied time period (Fig. 7). Raw data reach values as low and high as 0.2 °C and 6.6 °C, respectively. Average BWTs of ~3 °C are ~1.5 °C warmer than present-day deep-sea temperatures at that site (Locarnini et al., 2013), implying a ~1.5 °C cooling of EEP deep waters from ~2.5 Ma until today. This ~1.5 °C cooling is at the lower end of temperature data derived from model simulations that indicate a decrease of 2–3 °C in the deep EEP from the mid-Pliocene period towards pre-industrial times (Burls et al., 2017). Visual evaluation of our smoothed BWT record appears to indicate low-amplitude (<2 °C) glacial-interglacial variations across the entire investigated time period, which means that BWTs during pronounced (as indicated by positive excursions in the benthic $\delta^{18}O$ record) glacials of the iNHG (MIS 100, 98 and 96) are indistinguishable to less intense glacials of our study interval (MIS 104 and 102).

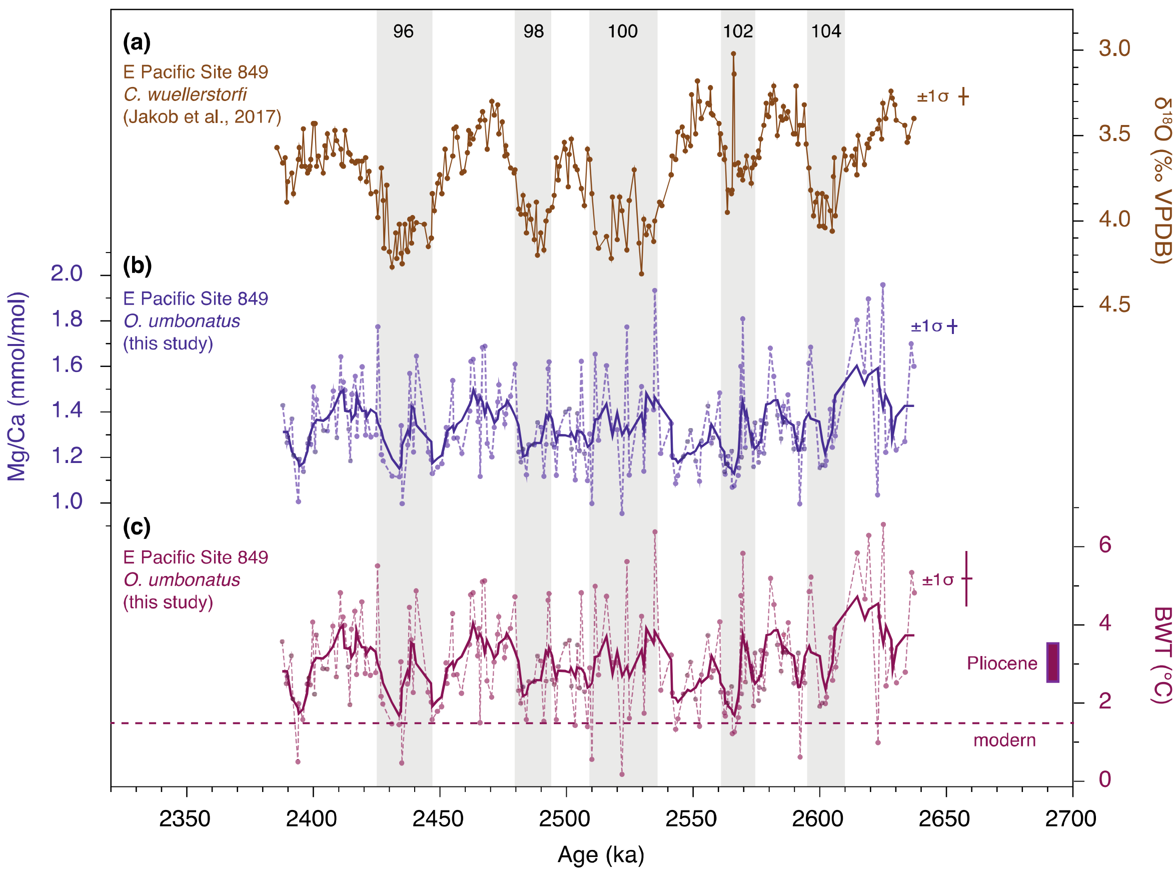

Figure 7. Proxy records for the deep East Pacific (Site 849) covering ~2.65–2.4 Ma (MIS G1–95). (a) Oxygen-isotope record of the benthic foraminifer *C. wuellerstorfi* for age control (Jakob et al., 2017). (b) Mg/Ca record derived from the benthic foraminifer *O. umbonatus*. (c) Mg/Ca-based estimates of deep-sea temperature (corrected for past changes in Mg/Ca_{sw}) in comparison to the modern value (dashed line, ~1.5 °C (Locarnini et al., 2013)) and modelled mid-Pliocene values (purple bar; calculated from the pre-industrial to mid-Pliocene BWT difference of 2–3 °C (Burls et al., 2017) and a pre-industrial North Pacific BWT value of ~0.5 °C (Hill et al., 2017)) at Site

849. Dashed lines in (b) and (c) show raw data, solid lines represent the five-point smoothed average of a record. Vertical bars indicate the standard deviation associated with the proxy records. Grey bars mark glacial periods.

3.2.2 Atlantic-Pacific difference

The only other deep-water temperature record for our study interval with a sufficient temporal resolution to compare with our new record from EEP Site 849 comes from North Atlantic Site U1313 (Jakob et al., 2020) and is based on exactly the same methodology applied herein. Site U1313 is a reoccupation of DSDP Site 607, for which a Mg/Ca-based BWT record is also available (Sosdian & Rosenthal, 2009). The temporal resolution of that record, is however, much lower (~3 kyr) compared to that of the BWT records from Site U1313 (~375–1500 yr) and Site 849 (~800 yr), such that peak glacial and interglacial values are possibly not captured in the lower resolved record from Site 607. In addition, the reliability of BWTs reconstructed for Site 607 has been questioned as modern values cannot be reconciled when applying the approach used by Sosdian & Rosenthal (2009) to core-top samples (Yu & Broecker, 2010). Importantly, the latter has been ensured for the approach used to reconstruct BWTs at Sites U1313 (Jakob et al., 2020) and 849 (Fig. 5)

At Site U1313, BWT raw data fluctuate between 3.8 °C and 11.1 °C and the smoothed record indicates temperatures between 4.4 °C and 9.5 °C. The average BWT value (6.9 °C) is clearly above the present-day deep-sea temperature at that site (~2.5 °C; Locarnini et al., 2013), and also 3.9 °C warmer compared to Plio-Pleistocene temperatures at EEP Site 849 (Fig. 8b). Average BWTs are also higher than the modelled mid-Pliocene deep-sea temperature of 3.1–3.4 °C at Site U1313 (Hill et al., 2017). The latter implies i) warming in the North Atlantic from the mid-Pliocene towards the Plio-Pleistocene transition, which is, however, difficult to reconcile with the general picture of global cooling from the mid-Pliocene to the present-day; ii) uncertainties in the Site U1313 BWT reconstruction, which is, however, unlikely as the robustness of this reconstruction has been proven with core-top samples (Jakob et al., 2020); or

iii) uncertainties associated with the model simulation, such as local palaeogeographic changes not being incorporated into the model (Hill et al., 2017).

The Atlantic-Pacific (Site U1313-to-849) BWT difference as outlined above was not constant during the studied interval, but varied on glacial-interglacial timescales. Specifically, ΔBWT was typically smaller than the average difference (3.9 °C) during strong glacials and larger during interglacials, which is related to larger-scale glacial-interglacial BWT amplitudes in the North Atlantic (>3 °C) compared to the EEP (<2 °C). We ascribe this discrepancy to changing deep-water masses with different temperatures that alternately influenced the seafloor in the North Atlantic on glacial-interglacial timescales, while the deep EEP was permanently bathed by a single water mass that ultimately derives from the high southern latitudes.

Supporting this view, our new ε_{Nd} data from Site 849 in the EEP show relatively constant values between -3.2 and -2.7 that are nearly identical to present-day values in this region (Hu and Piotrowski, 2018) (Fig. 8a), indicating the presence of only one water mass at that locality during both glacials and interglacials. In contrast, ε_{Nd} data from the same interval at Site U1313 in the North Atlantic (Lang et al., 2016) (Fig. 8a) suggest that the influence of northern-sourced waters, which prevailed during interglacials at that site, was suppressed during late Pliocene/early Pleistocene glacials; at those times, colder, southern-sourced waters advanced into the deep North Atlantic.

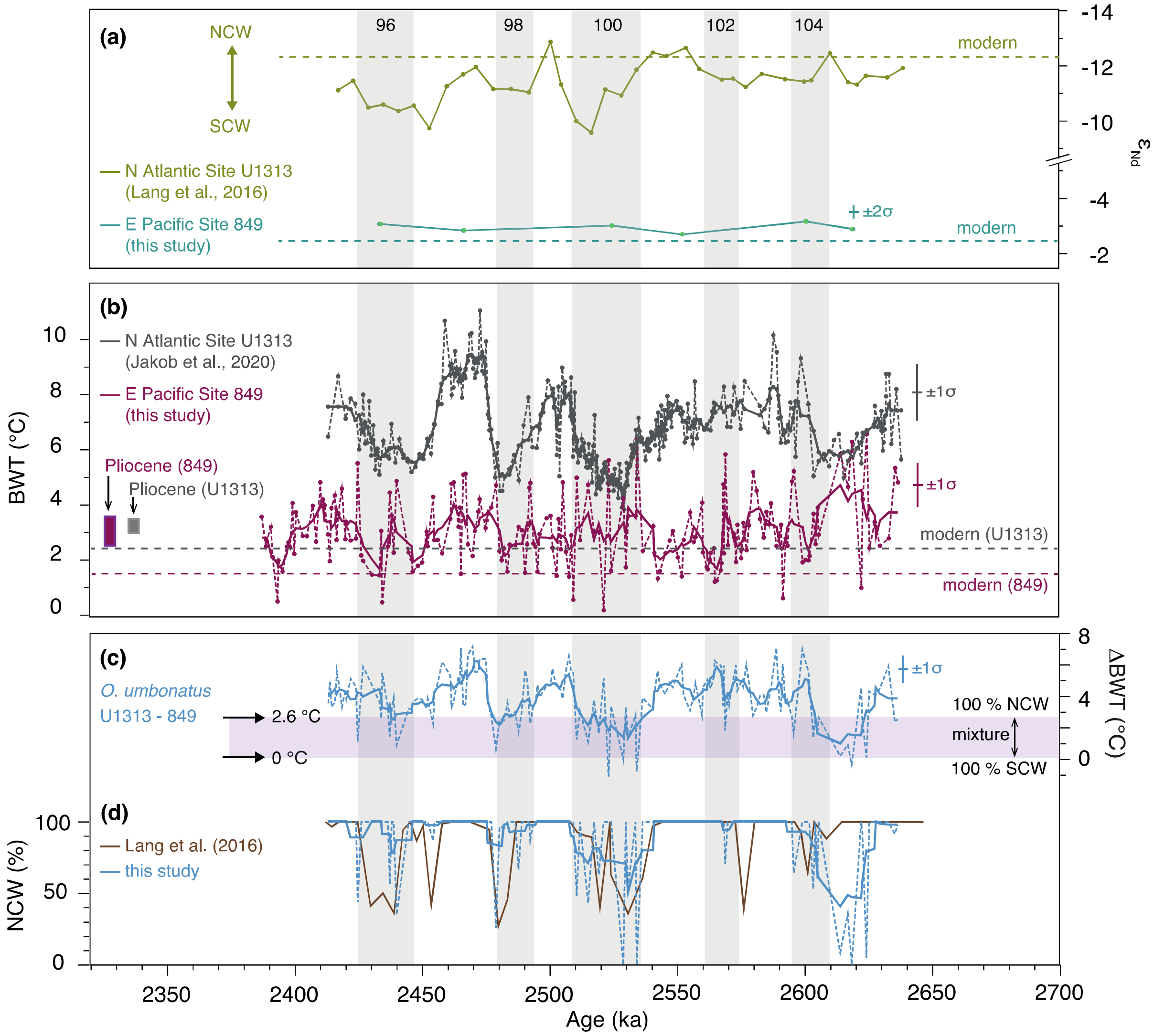

Figure 8. East Pacific and North Atlantic ε_{Nd} and deep-water temperature, together with estimates of northern-component waters at Site U1313 for ~2.65–2.4 Ma (MIS G1–95). (a) Fish-debris-derived ε_{Nd} record from Sites 849 (this study) and U1313 (Lang et al., 2016) with lower values indicating NCW and higher values indicating SCW. Dashed lines indicate modern ε_{Nd} values of NADW (-12.3; Tachikawa et al., 2017) and of bottom waters close to Site 849 (Site RC13-114; -2.5; Hu and Piotrowski, 2018). (b) *O. umbonatus*-derived deep-sea temperatures (Mg/Ca_{sw}-corrected) from Sites 849 (this study) and U1313 (Jakob et al., 2020) in comparison to i) modern BWTs (horizontal lines; Locarnini et al., 2013) of ~1.5 °C (Site 849) and ~2.5 °C (Site U1313), and ii) modelled BWTs for the mid-Pliocene (vertical bars) of 3.1–3.4 °C (Site U1313; Hill et al., 2017) and 2.5–3.5 °C (Site 849; see Fig. 7 for details and references). (c) Atlantic-Pacific temperature difference based on the BWT records shown in (b), purple bar marks a mixture between NCW and SCW based on their modern BWTs (Craig & Gordon, 1965). (d) ΔBWT-based estimates of %NCW (blue; this study) in comparison to a previous %NCW record derived from $\delta^{13}C$

(brown; Lang et al., 2016). Dashed lines in (b) and (c) indicate raw data, solid lines show a five-point smoothed average. Vertical grey bars mark glacial periods.

3.3 Deep-ocean circulation change in the North Atlantic across iNHG

Based on the Atlantic-Pacific (Site U1313-to-849) BWT difference, we calculated a record of relative changes between northern- and southern-sourced waters in the deep North Atlantic. As outlined in Section 2.6, our calculations assume BWT differences of 0 °C and 2.6 °C to correspond to 0 % and 100 % northern-sourced waters at Site U1313 (Fig. 8c).

Our new record of %NCW at Site U1313 (Fig. 8d) indicates different deep-water masses that alternately influenced the seafloor on glacial-interglacial timescales. In particular, we observe an increased influence of deep waters from the high southern latitudes at the expense of northern-sourced deep waters during prominent glacials of the iNHG. This pattern is generally consistent with previously published reconstructions for the same time interval (e.g., Raymo et al. 1990; Lang et al., 2016), but the higher temporal resolution of our new record reveals a much more detailed picture of prevailing water masses in the deep North Atlantic Ocean.

Incursions of southern-sourced waters were strongest in our record during glacial MIS 100, i.e., the first glacial during which the Laurentide Ice Sheet advanced into the midlatitudes (Balco and Rovey, 2010). Our calculations imply that during this glacial, NCW at Site U1313 was possibly (at least temporary) completely replaced by SCW. During MIS 98 and 96, i.e., the other two prominent glacials of the iNHG, SCW may have reached an amount of up to ~75 % at Site U1313. The potential temporal replacement of ~75–100 % of NCW by SCW, as implied by our calculation for strong iNHG glacials, is in the same order as estimates from Raymo et al. (1990) and Lang et al. (2016) for several glacials of the past 1 Myrs, except for the Last Glacial Maximum. During the latter, only ~35–55 % of NCW was likely replaced by SCW in the deep North Atlantic. Regardless of the magnitude of change, our records thus support the "traditional" view (see Section 1 for details; "changing mode" in Fig. 1a) on glacial-interglacial variations of North Atlantic northern- versus southern-sourced deep-water masses during the late Pliocene/early Pleistocene iNHG.

By extension, our detailed record even implies that glacials MIS 100, 98 and 96 were for the first time strong enough to invoke broader-scale changes in the deep-water circulation in the Atlantic Ocean. Previous studies (Lang et al., 2016; Sigman et al., 2010) suggest that excursions of SCW into the deep North Atlantic, as documented in our record, have important implications for the global carbon cycle, likely leading to increased storage of carbon dioxide in deep and cold southern-sourced waters. This then might have acted as a positive feedback mechanism through amplifying the strength of iNHG glacials.

The BWT difference we reconstruct also indicates a strong influence of southern-sourced waters in the deep North Atlantic during interglacial MIS G1 (Fig. 8c–d). This is, however, difficult to reconcile with evidence from both $\delta^{13}C$ (Lang et al., 2014) and ε_{Nd} (Lang et al., 2016) records for the prevalence of NCW at Site U1313 during this interglacial (Fig. 8a). The reduced BWT difference thus likely reflects regional (EEP) deep-sea warming as evidenced by unusually warm temperature spikes at Site 849 (i.e., the warmest BWTs that we reconstruct) rather than water-mass changes at Site U1313.

4. Implications for sea-level reconstructions from the North Atlantic

Our record of semi-quantitative estimates of northern- versus southern-sourced waters in the deep North Atlantic not only reveals detailed insights into ocean circulation in the deep North Atlantic during the iNHG. Perhaps even more importantly, it provides a unique opportunity to substantially improve geochemically-derived ($\delta^{18}O$ and Mg/Ca) sea-level reconstructions that are based on North Atlantic drill cores.

In this context, we integrated our new %NCW record with late Pliocene/early Pleistocene benthic Mg/Ca and $\delta^{18}O$ from Site U1313 to yield sea level and compared it to the originally published sea-level record (Jakob et al., 2020) (Fig. 9). The latter derived from a more hypothetical approach for water-mass correction (Dwyer and Chandler, 2008) compared to the usage of our new %NCW record for this purpose. In the “hypothetical approach”, a simple water-mass normalization factor is applied to the underlying Mg/Ca and $\delta^{18}O$ proxy records, which is based on a linear regression (BWT = 5 × $\delta^{18}O_{sw}$ + 2.6) between modern NADW (2.6 °C and 0.1‰) and AABW (0 °C and −0.5‰) temperature and $\delta^{18}O_{sw}$ endmembers (Craig & Gordon, 1965; Dwyer and Chandler, 2008).

Our resulting %NCW-derived sea-level curve (blue line in Fig. 9) is, within the error typically associated with $\delta^{18}O$- and Mg/Ca-derived sea-level reconstructions of ±20–30 m (e.g., Sosdian & Rosenthal, 2009; Jakob et al., 2020), indistinguishable to the originally published record (purple line in Fig. 9). However, our new %NCW record helps to resolve a more detailed picture of sea-level variability than revealed by the original sea-level record. For example, it records higher-amplitude variations for frequencies shorter than the orbital-scale change for specific intervals (e.g., MIS 100 and 96) compared to the previous reconstruction (Fig. 9). Also, the glacial-interglacial amplitude of sea-level change appears to be slightly enhanced (e.g., MIS 101 to 100) or reduced (e.g., MIS 98 to 97) in our %NCW-derived reconstruction than resulting from the original record.

Our new, semi-quantitative record on %NCW in the deep North Atlantic thus provides a promising new avenue towards generally more accurate sea-level reconstructions based on North Atlantic drill cores. The high temporal resolution of our record is particularly important for deciphering millennial-scale changes in sea-level and hence ice-volume dynamics and therefore climate variability in general.

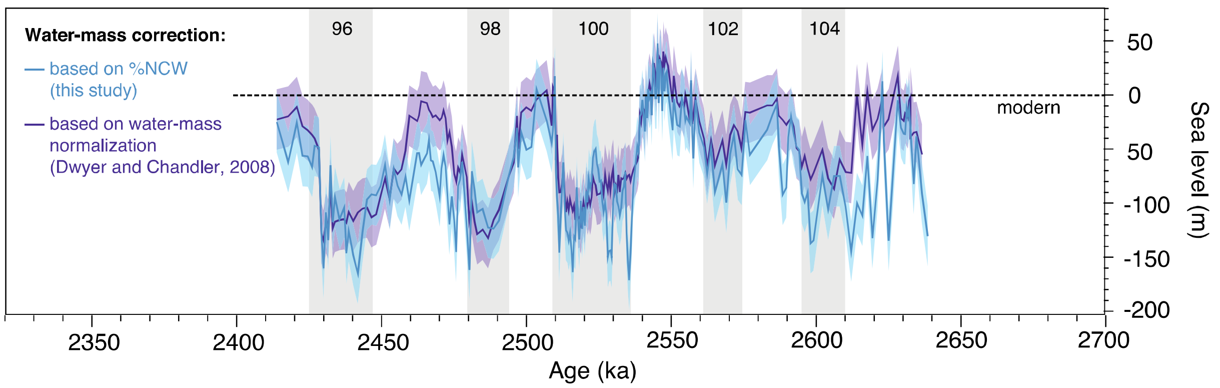

Figure 9. Application of our new %NCW record to reconstruct sea level in the North Atlantic for ~2.65–2.4 Ma (MIS G1–95). Mg/Ca- and $\delta^{18}O$-based sea-level data from North Atlantic Site U1313 (Jakob et al., 2020) corrected for changing deep-water masses using i) estimates of northern- versus southern-sourced deep waters at the same site (blue; this study) and ii) the more traditional approach for water-mass correction following Dwyer and Chandler (2008) (approach used in Jakob et al., 2020). Dashed line indicates modern sea level. Vertical grey bars mark glacial periods.

5. Summary and conclusions

We generated a new benthic foraminiferal Mg/Ca-based deep-sea temperature record together with a neodymium-isotope record for ODP Site 849 in the EEP across the late Pliocene/early Pleistocene iNHG (~2.65–2.4 Ma). We observe BWTs that were on average ~1.5 °C warmer than today and that only yield small-scale glacial-interglacial oscillations of <2 °C across the studied time interval. The new ε_{Nd} record indicates that the observed BWT variability is not related to changing deep-water masses, but rather reflects a pure temperature change of a single water mass.

We further used our new BWT record from the EEP to calculate the Atlantic-Pacific (Site U1313-to-849) deep-sea-temperature difference, which allowed to unravel the history of water-mass prevalence in the deep North Atlantic at a much higher temporal resolution than so far available. Based on the assumption of similar-to-modern deep-water-mass temperature differences, our record implies a relation between major glacials of the iNHG and changes in deep-water circulation pattern in the North Atlantic Ocean. In particular, our record shows an increased influence of deep waters from the high southern latitudes at the expense of northern-sourced deep waters during glacials, which was strongest during MIS 100. By extension, our record indicates that the iNHG glacials were likely strong enough to have a broader impact on the deep-water circulation in the Atlantic Ocean, with important implications for global carbon sequestration.

Moreover, we show that our semi-quantitative record of deep-water-mass change in the North Atlantic is of major importance for geochemically-based sea-level reconstructions that derive from North Atlantic drill cores. It provides a unique opportunity for correcting these records for changing deep-water masses at a so far unprecedented temporal resolution for a time interval that is widely considered a close analogue to near-future climate. As such, our record will help to increase our understanding of the Earth’s climate system in the past and, by extension, in the near future.

Acknowledgements

This research used samples provided by ODP and IODP, which are sponsored by the U.S. National Science Foundation and participating countries under the management of Joint Oceanographic Institutions, Inc. Silvia Rheinberger and Christian Scholz (Heidelberg University) are acknowledged for laboratory assistance during Mg/Ca measurements. Norbert Frank (Heidelberg University) is thanked for his support in neodymium isotope analysis. Hans-Peter Mayer and Alexander Varychev (Heidelberg University) are acknowledged for SEM assistance. Funding for this study was provided by the German Research Foundation (DFG, grants FR2544/2 and FR2544/6 to O.F., PR651/15 to J.P., and JA2803/2-1 to K.J.).

Declarations of competing interest

None.

References

Bailey, I., Bolton, C.T., DeConto, R.M., Pollard, D., Schiebel, R., Wilson, P.A., 2010. A low threshold for North Atlantic ice rafting from "low-slung slippery" late Pliocene ice sheets. Paleoceanography 25, PA1212, doi:1210.1029/2009PA001736.

Bailey, I., Hole, G.M., Foster, G.L., Wilson, P.A., Storey, C.D., Trueman, C.N., Raymo, M.E., 2013. An alternative suggestion for the Pliocene onset of major northern hemisphere glaciation based on the geochemical provenance of North Atlantic Ocean ice-rafted debris. Quaternary Science Reviews 75, 181–194.

Balco, G., Rovey, C.W., 2010. Absolute chronology for major Pleistocene advances of the Laurentide Ice Sheet. Geology 38, 795–798.

Barker, S., Greaves, M., Elderfield, H., 2003. A study of cleaning procedures used for foraminiferal Mg/Ca paleothermometry. Geochemistry Geophysics Geosystems 4, doi:10.1029/2003GC000559.

Barrientos, N., Lear, C.H., Jakobsson, M., Stranne, C., O'Regan, M., Cronin, T.M., Gukov, A.Y., Coxall, H.K., 2018. Arctic Ocean benthic foraminifera Mg/Ca ratios and global Mg/Ca-temperature calibrations: New constraints at low temperatures. Geochimica et Cosmochimica Acta 236, 240–259.

Böhm, E., Lippold, J., Gutjahr, M., Frank, M., Blaser, P., Antz, B., Fohlmeister, J., Frank, N., Andersen, M.B., Deininger, M., 2015. Strong and deep Atlantic meridional overturning circulation during the last glacial cycle. Nature 51, 73–76.

Bolton, C.T., Wilson, P.A., Bailey, I., Friedrich, O., Beer, C.J., Becker, J., Baranwal, S., Schiebel, R., 2010. Millennial-scale climate variability in the subpolar North Atlantic Ocean during the late Pliocene. Paleoceanography 25, PA4218, doi:4210.1029/2010PA001951.

Boyer, T.P., Antonov, J.I., Baranova, O.K., Coleman, C., Garcia, H.E., Grodsky, A., Johnson, D.R., Locarnini, R.A., Mishonov, A.V., O'Brien, T.D., Paver, C.R., Reagan, J.R., Seidov, D., Smolyar, I.V., Zweng, M.M., 2013. World Ocean Database 2013, in: S. Levitus and A. Mishonov (eds.), NOAA Atlas NESDIS 72, 209 pp.

Burls, N.J., Fedorov, A.V., Sigman, D.M., Jaccard, S.L., Tiedemann, R., Haug, G.H., 2017. Active Pacific meridional overturning circulation (PMOC) during the warm Pliocene. Science Advances 3, doi:10.1126/sciadv.1700156.

Cohen, A.S., O'Nions, R.K., Siegenthaler, R., Griffin, W.L., 1988. Chronology of the pressure-temperature history recorded by a granulite terrain. Contributions to Mineralogy and Petrology 98, 303–311.

Craig, H., Gordon, L.I., 1965. Deuterium and oxygen-18 variations in the ocean and the marine atmosphere. In Stable Isotopes in Oceanographic Studies and Paleotemperatures, edited by E. Tongiorgi, Spoletto, Pisa, Italy, pp. 9–130.

Curry, W.B., Oppo, D.W., 2005. Glacial water mass geometry and the distribution of $\delta^{13}C$ of ΣCO_2 in the western Atlantic Ocean. Paleoceanography 20, PA1017, doi:10.1029/2004PA001021.

de Boer, B., Lourens, L.J., van de Wal, R.S., 2014. Persistent 400,000-year variability of Antarctic ice volume and the carbon cycle is revealed throughout the Plio-Pleistocene. Nature Communications 5, doi:10.1038/ncomms3999.

Dwyer, G.S., Chandler, M.A., 2008. Mid-Pliocene sea level and continental ice volume based on coupled benthic Mg/Ca palaeotemperatures and oxygen isotopes. Philosophical Transactions of the Royal Society A: Mathematical, Physical and Engineering Sciences 367, 157–168.

Evans, D., Brierley, C., Raymo, M.E., Erez, J., Müller, W., 2016. Planktic foraminifera shell chemistry response to seawater chemistry: Pliocene-Pleistocene seawater Mg/Ca, temperature and sea level change. Earth and Planetary Science Letters 438, 139–148.

Expedition 306 Scientists (2006). Site U1313, in: North Atlantic climate, Proc. Integr. Ocean Drill. Program 303/306, doi:10.2204/iodp.proc.303306.112.2006.

Fantle, M. S., DePaolo, D.J., 2005. Variations in the marine Ca cycle over the past 20 million years. Earth and Planetary Science Letters 237, 102–117.

Fantle, M. S., DePaolo, D.J., 2006. Sr isotopes and pore fluid chemistry in carbonate sediment of the Ontong Java Plateau: Calcite recrystallization rates and evidence for a rapid rise in seawater Mg over the last 10 million years. Geochimica et Cosmochimica Acta 70, 3883–3904.

Ferreira, D., Cessi, P., Coxall, H.K., de Boer, A., Dijkstra, H.A., Drijfhout, S.S., Eldevik, T., Harnik, N., McManus, J.F., Marshall, D.P., Nilsson, J., Roquet, F., Schneider, T., Wills, R.C., 2018. Atlantic-Pacific Asymmetry in Deep-Water Formation: Annual Review of Earth and Planetary Sciences 46, 327–352.

Flesche Kleiven, H., Jansen, E., Fronval, T., Smith, T.M., 2002. Intensification of Northern Hemisphere glaciations in the circum Atlantic region (3.5–2.4 Ma) - ice-rafted detritus evidence. Palaeogeography, Palaeoclimatology, Palaeoecology 184, 213–223.

Ford, H.L., Sosdian, S.M., Rosenthal, Y., Raymo, M.E., 2016. Gradual and abrupt changes during the Mid-Pleistocene Transition. Quaternary Science Reviews 148, 222–233.

Frank, M., 2002. Radiogenic isotopes: Tracers of past ocean circulation and erosional input. Reviews of Geophysics 40, doi:10.1029/2000RG000094.

Gebbie, G., 2014. How much did Glacial North Atlantic Water shoal? Paleoceanography 29, 190–209, doi:10.1002/2013PA002557.

Greaves, M., Caillon, N., Rebaubier, H., Bartoli, G., Boharty, S., Cacho, I., Clarke, L., Cooper, M., Daunt, C., Delaney, M., deMenocal, P., 2008. Interlaboratory comparison study of calibration standards for foraminiferal Mg/Ca thermometry. Geochemistry Geophysics Geosystems 9, Q08010, doi:08010.01029/02008GC001974.

Hagelberg, T., Shackleton, N., Pisias, N., and Shipboard Scientific Party, 1992. Proceedings of the Ocean Drilling Program, Initial Reports 138, Ocean Drilling Program, College Station, Texas.

Hasenfratz, A.P., Schiebel, R., Thornalley, D.J.R., Schönfeld, J., Jaccard, S.L., Martínez-García, A., Holbourn, A., Jennings, A.E., Kuhnt, W., Lear, C.H., Marchitto, T.M., Quillmann, U., Rosenthal, Y., Yu, J., Haug, G.H., 2017. Mg/Ca-temperature calibration for the benthic foraminifera *Melonis barleeanum* and *Melonis pompilioides*. Geochimica et Cosmochimica Acta 217, 365–383.

Healey, S.L., Thunell, R.C., Corliss, B.H., 2008. The Mg/Ca-temperature relationship of benthic foraminiferal calcite: New core-top calibrations in the <4°C temperature range: Earth and Planetary Science Letters 272(3–4), doi:510.1016/j.epsl.2008.1005.1023.

Henry, L.G., McManus, J.F., Curry, W.B., Roberts, N.L., Piotrowski, A.M., Keigwin, L.D., 2016. North Atlantic ocean circulation and abrupt climate change during the last glaciation. Science 353, 470–474.

Hill, D.J., Bolton, K.P., Haywood, A.M., 2017. Modelled ocean changes at the Plio-Pleistocene transition driven by Antarctic ice advance. Nature Communications 8, doi:10.1038/ncomms14376.

Howe, J.N.W., Piotrowski, A.M., Noble, T.L., Mulitza, S., Chiessi, C.M., Bayon, G., 2016. North Atlantic Deep Water Production during the Last Glacial Maximum. Nature Communications 7, doi:10.1038/ncomms11765.

Hu, R., Piotrowski, A.M., 2018. Neodymium isotope evidence for glacial-interglacial variability of deepwater transit time in the Pacific Ocean. Nature Communications 9, doi: 10.1038/s41467-018-07079-z.

Jacobsen, S.B., Wasserburg, G.J., 1980. Sm-Nd isotopic evolution of chondrites. Earth and Planetary Science Letters 50, 139–155.

Jakob, K.A., Wilson, P.A., Bahr, A., Bolton, C.T., Pross, J., Fiebig, J., Friedrich, O., 2016. Plio-Pleistocene glacial-interglacial productivity changes in the eastern equatorial Pacific upwelling system. Paleoceanography 31, 453–470, doi:410.1002/ 2015PA002899.

Jakob, K.A., Bolton, C.T., Wilson, P.A., Bahr, A., Pross, J., Fiebig, J., Kähler, K., Friedrich, O., 2017. Glacial-interglacial changes in equatorial Pacific surface-water structure during the Plio-Pleistocene intensification of Northern Hemisphere Glaciation. Earth and Planetary Science Letters 463, 69–80, doi:10.1016/j.epsl.2017.1001.1028.

Jakob, K.A., Pross, J., Scholz, C., Fiebig, J., Friedrich, O., 2018. Thermocline state change in the eastern equatorial Pacific during the late Pliocene/early Pleistocene intensification of Northern Hemisphere Glaciation. Climate of the Past 14, 1079–1095.

Jakob, K.A., Wilson, P.A., Pross, J., Ezard, T.H.G., Fiebig, J., Repschläger, J., Friedrich, O., 2020. A new sea-level record for the Neogene/Quaternary boundary reveals transition to a more stable East Antarctic Ice Sheet. Proceedings of the National Academy of Sciences of the United States of America 117(49), 30980–30987, doi: 10.1073/pnas.2004209117.

Johnson, G.C., 2008. Quantifying Antarctic Bottom Water and North Atlantic Deep Water volumes. Journal of Geophysical Research 113, doi:10.1029/2007JC004477.

Keigwin, L.D., 2004. Radiocarbon and stable isotope constraints on Last Glacial Maximum and Younger Dryas ventilation in the western North Atlantic. Paleoceanography 19, PA4012, doi:10.1029/2004PA001029.

Knudson, K.P., Ravelo, A.C., 2015. North Pacific Intermediate Water circulation enhanced by the closure of the Bering Strait. Paleoceanography 30, 1287–1304.

Kroopnick, P.M., 1985. The distribution of ^{13}C of $\sum CO_2$ in the world oceans. Deep Sea Research 32, 57–84.

Kwiek, P.B., Ravelo, A.C., 1999. Pacific Ocean intermediate and deep water circulation during the Pliocene. Palaeogeography, Palaeoclimatology, Palaeoecology 154, 191–217.

Lang, D.C., Bailey, I., Wilson, P.A., Beer, C.J., Bolton, C.T., Friedrich, O., Newsam, C., Spencer, M.R., Gutjahr, M., Foster, G.L., Cooper, M.J., Milton, J.A., 2014. The transition on North America from the warm humid Pliocene to the glaciated Quaternary traced by eolian dust deposition at a benchmark North Atlantic Ocean drill site. Quaternary Science Reviews 93, 125–141.

Lang, D.C., Bailey, I., Wilson, P.A., Chalk, T.B., Foster, G.L., Gutjahr, M., 2016. Incursions of southern-sourced water into the deep North Atlantic during late Pliocene glacial intensification. Nature Geoscience 9, 375–379.

Lear, C.H., Rosenthal, Y., Slowey, N., 2002. Benthic foraminiferal Mg/Ca-paleothermometry: A revised core-top calibration. Geochimica et Cosmochimica Acta 66, 3375–3387.

Lear, C.H., Mawbey, E.M., Rosenthal, Y., 2010, Cenozoic benthic foraminiferal Mg/Ca and Li/Ca records: Toward unlocking temperatures and saturation states. Paleoceanography 25, PA4215, doi:10.1029/2009PA001880.

Lear, C.H., Coxall, H.K., Foster, G.L., Lunt, D.J., Mawbey, E.M., Rosenthal, Y., Sosdian, S.M., Thomas, E., Wilson, P.A., 2015. Neogene ice volume and ocean temperatures: Insights from infaunal foraminiferal Mg/Ca paleothermometry. Paleoceanography 30, doi:10.1002/ 2015PA002833.

Lisiecki, L.E., 2014. Atlantic overturning responses to obliquity and precession over the last 3 Myr. Paleoceanography 29, 71–86.

Lisiecki, L.E., Raymo, M.E., 2005. A Pliocene-Pleistocene stack of 57 globally distributed benthic $\delta^{18}O$ records. Paleoceanography 20, PA1003, doi:1010.1029/2004PA001071.

Locarnini, R.A., Mishonov, A.V., Antonov, J.I., Boyer, T.P., Garcia, H.E., Baranova, O.K., Zweng, M.M., Paver, C.R., Reagan, J.R., Johnson, D.R., Hamilton, M., Seidov, D., 2013. World Ocean Atlas 2013, in: S. Levitus and A. Mishonov (eds.), NOAA Atlas NESDIS 73, 40 pp.

Martin, E.E., Haley B.A., 2000. Fossil fish teeth as proxies for seawater Sr and Nd isotopes. Geochimica et Cosmochimica Acta 64, 835–847.

Mayer, L., Pisias, N., Janecek et al., T., 1992. Proceedings of the Ocean Drilling Program, Initial Reports 138, Ocean Drilling Program, College Station, Texas.

Miller, K.G., Browning, J.V., Schmelz, W.J., Kopp, R.E., Mountain, G.S., Wright, J.D., 2020. Cenozoic sea-level and cryospheric evolution from deep-sea geochemical and continental margin records. Science Advances 6, eaaz1346.

Mix, A.C., Pisias, N.G., Rugh, W., Wilson, J., Morey, A., Hagelberg, T.K., 1995. Benthic foraminifer stable isotope record from Site 849 (0–5 Ma): local and global climate changes. Proceedings of the Ocean Drilling Program, Scientific Results 138, 371–412.

Naafs, B.D.A., Hefter, J., Stein, R., 2013. Millennial-scale ice rafting events and Hudson Strait Heinrich(-like) Events during the late Pliocene and Pleistocene: a review. Quaternary Science Reviews 80, 1–28.

Paillard, D., Labeyrie, L., Yiou, P., 1996. Macintosh program perfroms time-series analysis. Eos, Transactions American Geophysical Union 77, doi:10.1029/1096EO00259.

Pin, C., Briot, D., Bassin, C., Poitrasson, F., 1994. Concomitant separation of strontium and samarium-neodymium for isotopic analysis in silicate samples, based on specific extraction chromatography. Analytica Chimica Acta 298, 209–217.

Pöppelmeier, F., Blaser, P., Gutjahr, M., Jaccard, S.L., Frank, M., Max, L., Lippold, J., 2020. Northern-sourced water dominated the Atlantic Ocean during the Last Glacial Maximum. Geology 48, 826–829.

Rahmstorf, S., 2002. Ocean circulation and climate during the past 120,000 years. Nature 419, 207–214.

Rathmann, S., Kuhnert, H., 2008. Carbonate ion effect on Mg/Ca, Sr/Ca and stable isotopes on the benthic foraminifera *Oridorsalis umbonatus* off Namibia. Marine Micropaleontology 66, 120–133.

Rausch, S., Böhm, F., Bach, W., Klügel, A., Eisenhauer, A., 2013. Calcium carbonate veins in ocean crust record a threefold increase of seawater Mg/Ca in the past 30 million years. Earth and Planetary Science Letters 362, 215–224.

Raymo, M.E., Ruddiman, W.F., Shackleton, N.J., Oppo, D.W., 1990. Evolution of Atlantic-Pacific $\delta^{13}C$ gradients over the last 2.5 m.y. Earth and Planetary Science Letters 97, 353–368.

Raymo, M.E., Hodell, D., Jansen, E., 1992. Response of deep ocean circulation to initiation of Northern Hemisphere glaciation (3–2 Ma). Paleoceanography 7, 645–672.

Raymo, M., Ganley, K., Carter, S., Oppo, D., McManus, J., 1998. Millennial-scale climate instability during the early Pleistocene epoch. Nature 392, 699-702.

Reuss, A.E., 1851. Über die fossilen Foraminiferen und Entomostraceen der Septarienthone der Umgegend von Berlin. Zeitschrift der Deutschen Geologischen Gesellschaft 3, 49–92.

Rosenthal, Y., Perron-Cashman, S., Lear, C.H., Bard, E., Barker, S., Billups, K., Bryan, M., Delaney, M.L., 2004. Interlaboratory comparison study of Mg/Ca and Sr/Ca measurements in planktonic foraminifera for paleoceanographic research. Geochemistry Geophysics Geosystems 5, Q04D09.

Schlitzer, R., 2016. Ocean Data View, http://odv.awi.de.

Shackleton, N.J., Backman, J., Zimmerman, H., Kent, D.V., Hall, M., Roberts, D., Schnitker, D., Baldauf, J., Desprairies, A., Homrighausen, R., 1984. Oxygen isotope calibration of the onset of ice-rafting and history of glaciation in the North Atlantic region. Nature 307, 620–623.

Sigman, D.M., Hain, M.P., Haug, G.H., 2010. The polar ocean and glacial cycles in atmospheric CO_2 concentration. Nature 466, 47–55.

Sosdian, S., Rosenthal, Y., 2009. Deep-sea temperature and ice volume changes across the Pliocene-Pleistocene climate transitions. Science 325, 306–310.

Staudigel, H., Doyle, P., Zindler, A., 1985. Sr and Nd isotope systematics in fish teeth. Earth and Planetary Science Letters 76, 45–56.

Tachikawa, K., Arsouze, T., Bayon, G., Bory, A., Colin, C., Dutay, J.-C., Frank, N., Giraud, X., Gourlan, A.T., Jeandel, C., Lacan, F., Meynadier, L., Montagna, P., Piotrowski, A.M., Plancherel, Y., Pucéat, E., Roy-Barman, M., Waelbroeck, C., 2017. The large-scale evolution of neodymium isotopic composition in the global modern and Holocene ocean revealed from seawater and archive data. Chemical Geology 457, 131–148.

Tanaka, T., Togashi, S., Kamioka, H., Amakawa, H., Kagami, H., Hamamoto, T., Yuhara, M., Orihashi, Y., Yoneda, S., Shimizu, H., Kunimaru, T., Takahashi, K., Yanagi, T., Nakano, T., Fujimaki, H., Shinjo, R., Asahara, Y., Tanimizu, M., Dragusanu, C., 2000. JNdi-1: a neodymium isotopic reference in consistency with LaJolla neodymium. Chemical Geology 168, 279–281.

Tisserand, A.A., Dokken, T.M., Waelbroeck, C., Gherardi, J.-M., Scao, V., Fontanier, C., Jorissen, F., 2013. Refining benthic foraminiferal Mg/Ca-temperature calibrations using core-tops from the western tropical Atlantic: Implication for paleotemperature estimation. Geochemistry, Geophysics, Geosystems 14(4), 929–946.

Yu, J., Broecker, W.S., 2010. Comment on "Deep-sea temperature and ice volume changes across the Pliocene-Pleistocene climate transitions". Science 328, doi:10.1126/science.1186544.

Conflict of Interest

Declaration of interests

☒ The authors declare that they have no known competing financial interests or personal relationships that could have appeared to influence the work reported in this paper.

☐The authors declare the following financial interests/personal relationships which may be considered as potential competing interests:

Author statement

Kim A. Jakob: Investigation; Writing - Original Draft; Writing - Review & Editing; Visualization

Jörg Pross: Writing - Original Draft; Writing - Review & Editing

Jasmin M. Link: Investigation; Writing - Original Draft; Writing - Review & Editing

Patrick Blaser: Writing - Original Draft; Writing - Review & Editing

Anna Hauge Braaten: Investigation; Resources

Oliver Friedrich: Writing - Original Draft; Writing - Review & Editing; Supervision

Dataset (Table A.1)